Heat Generation Ability of Ferromagnetic Implants in Hyperthermia

Heat Generation Ability of Ferromagnetic Implants in Hyperthermia

Behrooz Rezaeealam[1,2], Sotoshi Yamada[1] and Yoshio Ikehata[1]

[1]Division of Biological Measurement and Applications, Institute of Nature and Environmental Technology, Kanazawa University, Kanazawa 920-1192 Japan
[2]Department of Electrical Engineering, Lorestan University, Khorramabad, P.O. Box 465, Iran

In this paper, proposed implants in literature are compared in terms of the ability to heat generation in electromagnetic thermotherapy. To destroy the tumor cells, their temperature must rise above 42.5°C. The magnitude of the temperature rise depends strongly on the thermal conductivity of the tissue that has not been considered in most studies. For this reason, liver tissue is modeled using bioheat transfer equation that is coupled to the electromagnetic equations and electrical circuits by employing Multiphysics finite element package COMSOL, in order to create the numerical model of the system.

***Index Terms*—Bioheat equation, Electromagnetic thermotherapy, Finite element method.**

I. Introduction

HYPERTHERMIA is a procedure for treatment of cancerous tumor by raising its temperature and there is a spectrum of ways of local intracorporal heat generation using focused microwave radiation, capacitive or inductive coupling of RF fields, implanted electrodes, focused ultrasound, or lasers. Recently, researchers are looking to employ electromagnetic thermotherapy as a treatment with no major side effects in comparison with various established treatments, such as surgical resection, radiation therapy and chemotherapy.

The hyperthermia using ferromagnetic implants has been reported in several studies for local warming of body tissues [1,2]. Also, as an alternative therapy, magnetic particle (MP) hyperthermia is a method where MPs are deposited in tumor tissue with subsequent heating by means of an external alternating magnetic field [3]. Although magnetic nanoparticles represent very promising systems due to their multifunctional capabilities, however, solid ferromagnetic implants have recently been shown to display higher efficiency rates than iron oxide nanoparticles [4].

Radiofrequency ablation (RFA) is regarded as a powerful and effective technique by which an ac current (usually 460-500kHz) is conducted by the RFA probe to flow through the tissue such that the local temperature can be raised rapidly and efficiently (about 90-110°C) to cause thermal ablation. However, the cost of the RFA probe is relatively high and it must overcome the blood coagulation issue because the blood clots may act as highly resistive objects that reduce the desired heating effect [5]. Meanwhile, RFA is not suitable for coagulate the main blood vessels in an organ since there is a heat-sink effect.

Alternatively, microwave ablation is relatively expensive and difficult to be applied for bloodless resection of tissues, since the area affected by the microwave ablation is limited to only about 2 cm away from the microwave probe [6].

The main advantage of hyperthermia using ferromagnetic implants is heating repeatedly the target tissue at lower temperature zone than that for RFA therapy [7]. In literature, several types of implants for hyperthermia have been proposed such as materials with low curie temperature [8,9], ferromagnetic core on which a coil is wound and connected to a chip capacitor [10] and also stainless steel needles [11,7]. The selection criterion of implants is their heat generation ability; however, the effectiveness of all types of implants has not been tested in vitro or in vivo experiment. In [12], implant of magnesium ferrite has been proposed that under an alternating magnetic field can achieve a temperature beyond 60°C for the first time.

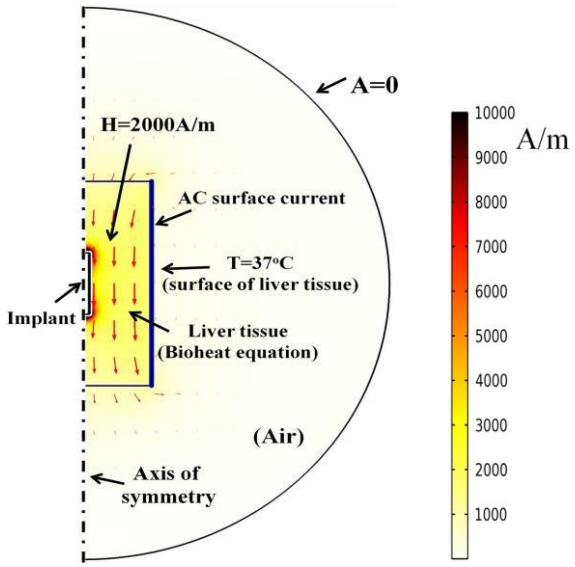

Fig. 1. Two-dimensional model of the heating problem.

Irreversible cell injury occurs when cells are heated to 460C for 60 minutes and with increasing temperatures the time necessary to induce cell death is shortened and at 60-1000C cell death is immediate and irreversible.

In this work, a numerical model is developed as shown in Fig.1, that can be used to evaluate the temperature rise in the tissue when exposed to high frequency magnetic field, and also a comparative study of heat generation for different configurations of implants is done.

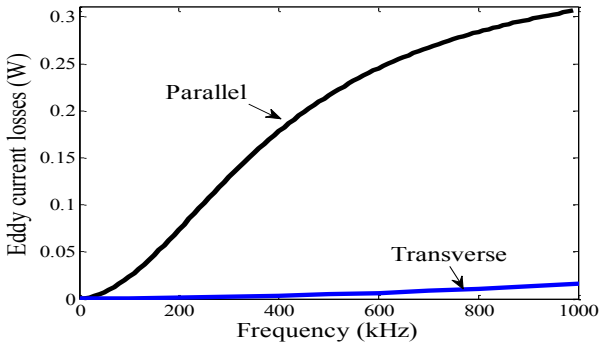

Fig. 2. Heat generation in stainless rods parallel and transverse to the external magnetic field (μ_r=400, σ=1.7e7 S/m).

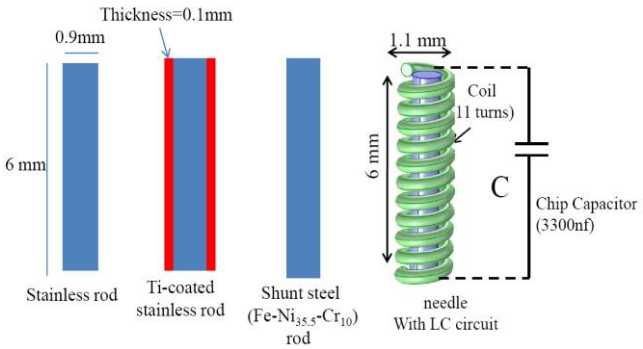

Fig. 3. Implant configurations with aspect ratio around 6.

II. Finite Element Model

The model approximates the body tissue with a large cylinder and assumes that its boundary temperature remains at 37°C during the entire procedure as depicted in Fig. 1. The tumor is located near the center of the cylinder and has the same thermal properties as the surrounding tissue. The model locates the ferromagnetic implant along the cylinder's center line.

The bioheat equation governs heat transfer in the tissue to determine the time-varying temperature distribution T that is caused by induced eddy currents:

$$\rho C_p \frac{\partial T}{\partial t} - \nabla \cdot k \nabla T = Q \tag{1}$$

where ρ=1050 is the density (kg.m^{-3}) of liver tissue, C_p=3600 is the specific heat (J.kg-^{1}.°C^{-1}), k=0.5 is the thermal conductivity (W.m^{-1}.°C^{-1}), and Q is the power density (W.m^{-3}) dissipated by the induced eddy currents in either liver tissue or the ferromagnetic implant. We neglect the heat generated by metabolic processes and the heat exchange due to blood perfusion in soft biological tissues since they are small compared with Q.

The heat source Q in (1) is given by:

$$Q = \frac{1}{2}\sigma |E|^2 \tag{2}$$

where σ=0.575e6 is the electrical conductivity (S.m^{-1}) and E is the electric field intensity (V.m^{-1}), governed by:

$$(jw\sigma - w^2\varepsilon)E + \nabla \times (\frac{1}{\mu}\nabla \times E) = -jwJ \tag{3}$$

Here, w is the angular frequency (rad.s^{-1}), ε is the permittivity (F.m^{-1}), μ is the permeability (N.A^{-2}), and J is the external current density (H.m^{-1}).

We employ Multiphysics finite element package (COMSOL) to perform finite element analysis on the temperature distribution T [13]. Electromagnetic field equations are solved in frequency domain, while the bioheat equation is solved in time domain, and for numerical stability, we set the time step size of the bioheat equation to 0.001 s, also, both the absolute and the relative tolerance of the solver are set to 1e-6.

We approximate the test system as a ferromagnetic implant exposed to a uniform magnetic field and an axisymmetric model is used since the excitation field is in parallel to the axis of the implant as shown in Fig. 1. It is worth noting that this is a conservative model since the orientation also corresponds to maximum heating that could possibly be generated in the tissue. Heat generation in stainless rods for both inclinations of parallel and transverse to the external magnetic field has been compared in Fig. 2, that shows the effect of shape-induced magnetic anisotropy, which is closely related to the value of the demagnetization field coefficient, and causes an undesirable effect on the heat generation ability in an ac magnetic field.

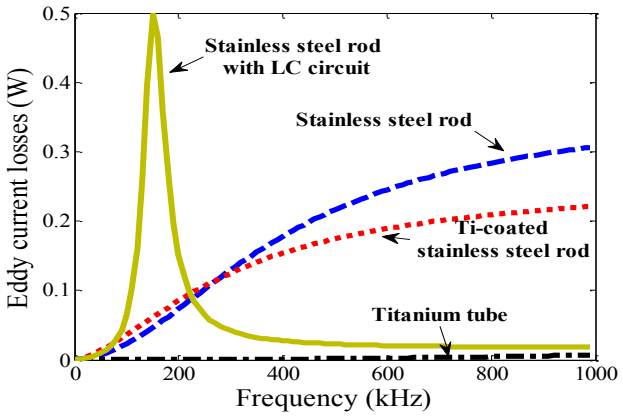

Fig. 4. Heat generation in different implant configurations, parallel to the external magnetic field (without considering heat transfer equations).

III. Implant Configurations

Of several types of implants employed in electromagnetic thermotherapy, four are compared. They are stainless-steel rod [4,7], Ti-coated stainless-steel rod [11], rod of shunt steel with low curie temperature [8,9] and stainless steel rod on which a coil of 11 turns, is wound and connected to a chip capacitor of 3300 nF (LC-type) [10] as illustrated in Fig. 3. Heat generation in the above mentioned implants is depicted in Fig. 4 that shows the eddy current losses versus the frequency of the external magnetic field, without considering heat transfer equations. It is observed that hollow Titanium tube produces much lower heat than the one of Ti-coated stainless steel rod and the results demonstrate the necessity of the magnetic core to improve the heat generation. Also, Fig. 4 shows that the LC-type implant has the highest heat generation ability at the resonance frequency of 155 kHz.

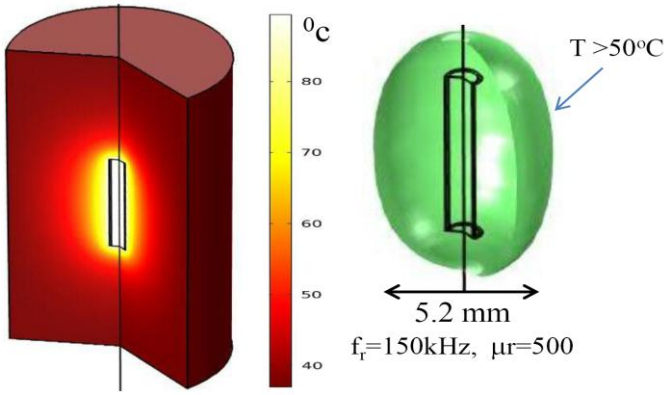

Fig. 5. Temperature distribution around the LC-type implant inside the liver tissue.

IV. Comparative Study of Heat Generation Ability of Implants

Fig. 5 shows the temperature distribution around the LC-type implant by considering the relative permeability of 500 for the magnetic core and the corresponding resonance frequency of 150 kHz. Furthermore, Fig. 5 shows the region where the temperature has reached at least 50 ^{0}C and cancer cells die. Fig. 6 shows the temperature rises on the surface of the LC-type implant in the first 200 s. It is evident that an increase in the magnetic core's relative permeability causes a slight reduction in the resonance frequency and also improves the temperature rise. It is worth mentioning that the ac surface current around the cylinder has been adjusted such that a uniform magnetic field of 1600 A/m (2 mT) is generated inside the cylinder.

For two-dimensional numerical mode, the coil around the needle could be modeled using multi-turn coil domain in COMSOL and it is coupled to the external electrical circuit. However, if the implant is not parallel to the external magnetic field, then a 3D model must be taken into account, while in 3D models, multi-turn coil domain is not available in COMSOL. Therefore, the coil is modeled as a wire that is wound around its magnetic core as shown in Fig. 7 and the related equations of electric current are added to the model and then both ends of the wire are connected to the external electrical circuit. Fig. 7 shows the temperature distribution inside the LC-type implant and also the current density flowing through the wire.

The relative permeability of stainless steel is set to 409 and Fig. 8 shows the temperature in the vicinity of implants. The LC-type implant increases the implant temperature up to 86^{o}C at the resonance frequency of 155kHz. Also, it is observed that Titanium-coated stainless rod has lower heat generation ability than the one of stainless alone. The implants are of 1mm in diameter and 6mm in length.

Soft-heating using implants with low curie temperature seems to be a suitable method for hyperthermia, as it regulates the temperature around the curie temperature [2,8,9]. Here, the shunt steel consisting of Fe, Ni 35.5% and Cr 10% has been investigated as thermosensitive magnetic materials with acute drop in the relative permeability at curie temperature of 75degC as shown in Fig. 9.

Fig. 10 shows the required frequency and magnetic flux

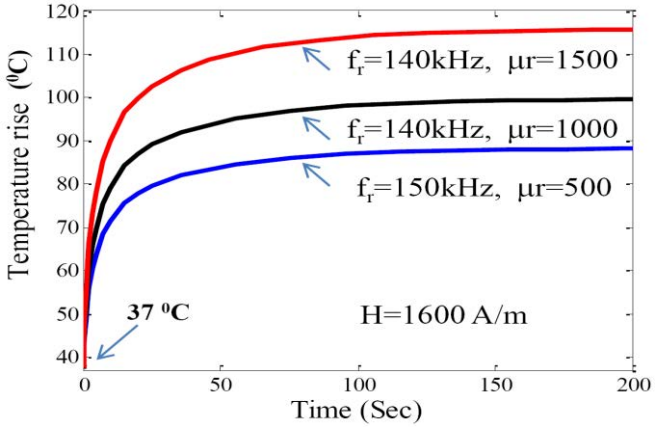

Fig. 6. Temperature rises in the first 200 s for different values of relative permeability of magnetic core (LC-type).

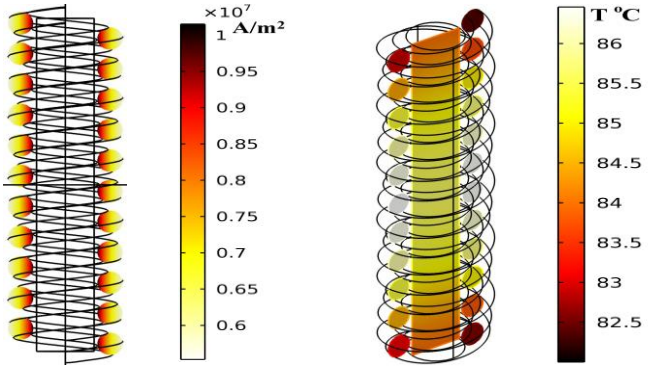

Fig. 7. Temperature distribution inside the LC-type implant and the current density flowing through the wire.

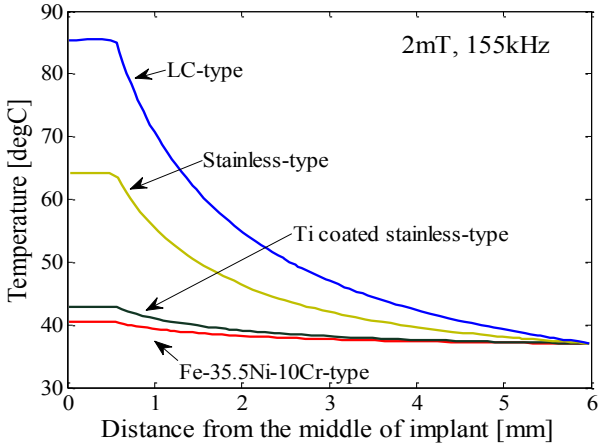

Fig. 8. Temperature rise around the implant inside the tissue.

density in order to increase the implant temperature up to its curie point of 75^{o}C. Materials with curie temperature below 200^{o}C, have low permeability and therefore to produce sufficient heat, they need a higher magnetic flux density or a higher exciting frequency in comparison with other type of implant such as stainless steel.

Fig. 11 shows the implants temperatures versus inclination angle at the same condition of B=2 mT and f=155kHz. It is obvious that the heat generation of implants is sensitive to the inclination angle and the LC-type has the highest sensitivity to the inclination angle.

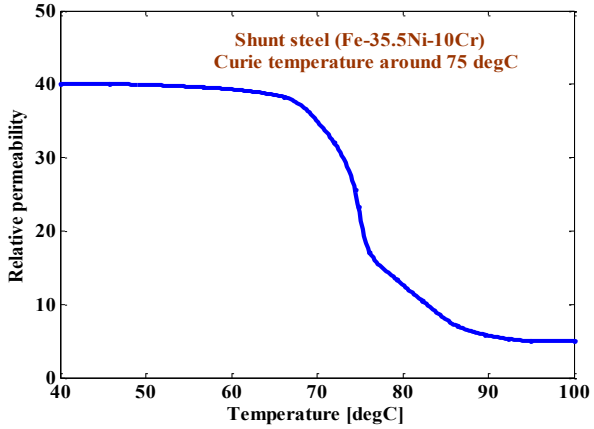

Fig. 9. The relative permeability versus temperature.

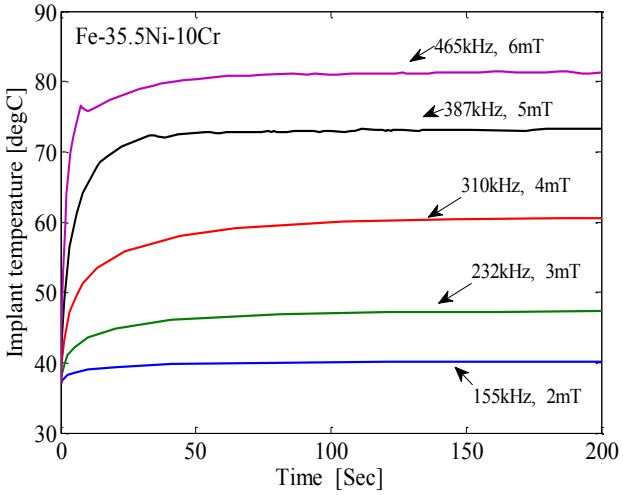

Fig. 10. Temperature characteristics of magnetic shunt steel.

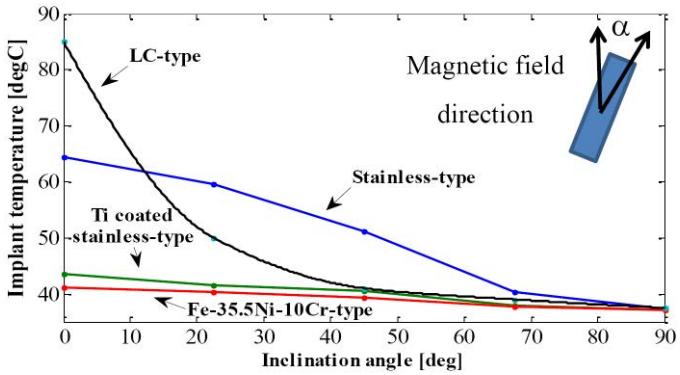

Fig. 11. Implants temperatures versus inclination angle (B=2 mT and f=155kHz).

V. Conclusion

A numerical model has been developed that can be used to evaluate the temperature rise inside the biological tissue caused by ferromagnetic implants when exposed to ac magnetic fields. The shape-induced magnetic anisotropy affects the heat generation of implants and the difference between the parallel and transverse oriented implants in heat generation is remarkable. Also, the numerical results show the Ti-coated implants produce less temperature than stainless steel implants in liver tissue for ablation therapy.

Materials with curie temperature below 200°C, need a higher magnetic flux density or a higher exciting frequency to produce sufficient heat in comparison with other type of implant such as stainless steel, because of lower permeability. The LC-type implant provides sufficient temperature in liver tissue to kill cancer cells, however, the heat generation of needle implants is sensitive to the inclination angle and it is recommended to employ distributed small size flakes in order to uniform heating.

References

[1] T. C. Cetas, A. M. Fletcher, D. W. Deyoung, M. W. Dewhirst, J. R. Oleson, R. B. Roemer, "Observations on the Use of Ferromagnetic Implants for Inducing Hyperthermia," *IEEE Trans. Biomedical Engineering*, vol. 31, no.1, pp. 76-90, 1984.

[2] T. Satoh, K. Murakami, T. Hoshino, T. Yanada and S. Kikuchi, "Local hyperthermia based on soft heating method utilizing temperature-sensitive ferrite rod," *IEEE Trans. Magn.*, vol. 26, no. 5, pp. 1551-1553, 1990.

[3] C. S. S. R. Kumar and F. Mohammad, "Magnetic nanomaterials for hyperthermia–based therapy and controlled drug delivery," *Advanced Drug Delivery Reviews*, vol. 63, pp. 789-808, 2011.

[4] R. Zuchini, H.-W. Tsai, C.-Y. Chen, C.-H. Huang, S.-C. Huang, G.-B. Lee, C.-F. Huang and X.-Z. Lin, "Electromagnetic thermotherapy using fine needles for hepatoma treatment," *Eur. J. Surg. Oncol.,* vol. 37, pp. 604-610, 2011.

[5] S. N. Goldberg, G. S. Gazelle, C. C. Compton, P. R. Mueller and K. K. Tanabe, "Treatment of intrahepatic malignancy with radiofrequency ablation," *Radiol. Pathol. Correlat.*, vol. 88, pp. 2452-2463, 2001.

[6] C. J. Simon, D. E. Dupuy and W. W. Mayo-smith, "Micowave ablation: principles and applications," *Radio Graphics*, vol. 25, pp. 69-83, 2005.

[7] S. C. Huang, Y. Y. Chang, Y. J. Chao, Y. S. Shan, X. Z. Lin and G. B. Lee, "Dual-row needle arrays under an electromagnetic thermotherapy system for bloodless liver resection surgery," IEEE *Trans. Biomed. Eng.*, vol. 59, no. 3, pp. 824-831, 2012.

[8] J. Oya, H. Shoji, F. Sato, H. Matsuki, S. Satomi, Y. Nihei, Y. Kurokawa, and T. Sato, "Thermotherapy with Metallic Stent Excited by the Magnetic Field," *IEEE Trans. Magn.*, vol. 42, no. 10, pp. 3593-3595, 2006.

[9] H. Matsuki, K. Murakami, T. Satoh and T. Hoshino, "An optimum design of a soft heating system for local hyperthermia," *IEEE Trans. Magn.*, vol. 23, no. 5, pp. 2440-2442,1987.

[10] K. Watabe, K. Kumagai, R. Matsumura, T. Yamada, T. Sato and Y. Takemura, "Hyperthermia implant consisting of resonant circuit delivered to tumor through 18G needle," *IEEE Trans. Magn.*, vol. 47, no. 10, pp. 2887-2889, 2011.

[11] T. Naohara, H. Aono, H. Hirazawa, T. Maehara, Y. Watanabe and S. Matsumoto, "Heat generation ability in AC magnetic field of needle-type Ti-coated mild steel for ablation cancer therapy," *COMPEL*, vol. 30, no. 5, pp. 1582-1588, 2011.

[12] K. Sato, Y. Watanabe, A. Horiuchi, S. Yukumi, T. Doi, M. Yoshida, Y. Yamamoto, N. Tsunooka and K. Kawachi, "Feasibility of new heating method of hepatic parenchyma using a sintered $MgFe_2O_4$ needle under an alternating magnetic field," *Journal of Surgical Research*, vol. 146, pp. 110-116, 2008.

[13] COMSOL, MULTIPHYSICS © (FEMLAB), [online]. http://www.comsol.com